

# On quenches in non-integrable quantum many-body systems: the one-dimensional Bose-Hubbard model revisited

Guillaume Roux<sup>1,2,\*</sup>

<sup>1</sup>*LPTMS, Université Paris-Sud, CNRS, UMR 8626, 91405 Orsay, France.*

<sup>2</sup>*Institute for Theoretical Physics C, RWTH Aachen University, D-52056 Aachen, Germany.*

(Dated: June 21, 2024)

When a quantum many-body system undergoes a quench, the time-averaged density-matrix  $\bar{\rho}$  governs the time-averaged expectation value of any observable. It is therefore the key object to look at when comparing results with equilibrium predictions. We show that the weights of  $\bar{\rho}$  can be efficiently computed with Lanczos diagonalization for large Hilbert spaces, giving a systematic method for studying quenches. As an application, the non-integrable Bose-Hubbard model is shown to display two regimes: one with an approximate Boltzmann distribution for small quench amplitudes, and one where the distributions do not follow standard equilibrium predictions. Some thermodynamics features of  $\bar{\rho}$ , like the energy fluctuations and the entropy, are also discussed.

PACS numbers: 05.70.Ln, 75.40.Mg, 67.85.Hj

Recent experiments [1] in ultra-cold atoms have renewed the interest for the time-evolution of an isolated quantum many-body system after a sudden change of the Hamiltonian parameters, the so-called “quantum quench”. Many questions arise from such a setup, among which the relaxation to equilibrium statistics, the memory kept from the initial state, and the role of the integrability of the Hamiltonian. Analytical and numerical results support different answers to these questions [2, 4, 5, 6, 7], though most observed that observables do not follow equilibrium predictions. As it has been pointed out [7], looking at simple observables, yet experimentally accessible, might not be considered as sufficient to fully address these questions. As time-evolution is unitary, there is no relaxation in the sense of a stationary density-matrix, contrary to what can happen in a subsystem [8]. However, observables will fluctuate around some average. Standard definitions show that the time-averaged density-matrix  $\bar{\rho}$  of the system governs any observable and its fluctuations. It is therefore desirable to have a systematic way of getting some information about  $\bar{\rho}$ .

In this paper, we show how Lanczos diagonalization (LD) can allow for the calculation of the weights of the time-averaged density-matrix. This method works for both integrable and non-integrable models, and gives access to large Hilbert spaces. As an application, the example of a quench in the one-dimensional Bose-Hubbard model (BHM) [4] is revisited, and it is shown that there is two distinct regimes depending on the quench amplitude. In the perturbative regime of the quench amplitude, an approximate Boltzmann law is found, while distributions that do not belong to equilibrium ensembles emerge for large quenches. Lastly, we show that  $\bar{\rho}$  bears some memory of the initial state through energy fluctuations and entropy.

We start by recalling [9] and introducing some definitions that hold for finite size systems. At time  $t < 0$ , the Hamiltonian is denoted by  $\mathcal{H}_0$  and its eigenvectors and eigenvalues by  $|\psi_n\rangle$  and  $E_n$ . The system is prepared in some state  $|\psi_0\rangle$ , that usually is the ground-state of  $\mathcal{H}_0$ . At  $t = 0$ , the Hamiltonian is changed to  $\mathcal{H}$  which eigenvalues and eigenvectors are  $\omega_n$  and  $|\phi_n\rangle$ . Then, the time-evolving density-matrix

of the whole system reads  $\rho(t) = \sum_n p_n |\phi_n\rangle \langle \phi_n| + \sum_{n < m} \sqrt{p_n p_m} [e^{-i\Omega_{nm}t + i\Theta_{nm}} |\phi_n\rangle \langle \phi_m| + h.c.]$ , with  $\Theta_{nm} = \theta_n - \theta_m$  and  $\theta_n = \text{Arg} \langle \phi_n | \psi_0 \rangle$ , and  $\Omega_{nm} = \omega_n - \omega_m$ .  $p_n = |\langle \psi_0 | \phi_n \rangle|^2$  are the diagonal weights of the density-matrix, that are directly determined by the initial state and satisfy  $\sum_n p_n = 1$ . As we are interested in the time-averaged expectation value of an observable  $O$ , we define  $\bar{O} = \lim_{t \rightarrow \infty} \frac{1}{t} \int_0^t \text{Tr}[\rho(s)O] ds = \sum_n p_n O_{nn}$ , with the matrix elements  $O_{nm} = \langle \phi_n | O | \phi_m \rangle$ . Interestingly, averaging  $\langle O \rangle_0$  (with  $\langle \cdot \rangle_0 = \langle \psi_0 | \cdot | \psi_0 \rangle$ ) over random initial phase differences  $\Theta_{nm}$  gives back  $\bar{O}$ , relating the time-averaging to the loss of information on the initial phases. Similarly, by averaging the time-evolving density-matrix, one gets

$$\bar{\rho} = \sum_n p_n |\phi_n\rangle \langle \phi_n| ,$$

which governs any time-averaged observable since  $\bar{O} = \text{Tr}[\bar{\rho}O]$ . Furthermore, it has been very recently shown [10] that  $\bar{\rho}$  is the experimentally relevant object to look at, and that the  $p_n$  weights enter in the microscopic expression of the work and heat done on the system in the quench [11]. Note that the evolving state is a pure state so its von Neumann entropy  $S[\rho] = -\text{Tr}[\rho \ln \rho]$  is zero, while  $S[\bar{\rho}]$  is non-zero due to the loss of information induced by time-averaging. In addition to time-averaged observables, one must also look at their time-averaged fluctuations  $\Delta O = [\text{Tr}[\bar{\rho}(O - \bar{O})^2]]^{1/2}$ . If  $O$  is diagonal in the  $|\phi_n\rangle$  basis, like the energy  $\mathcal{H}$ , the time-averaged expectations and fluctuations are fixed by the initial state:  $\bar{O} = \langle O \rangle_0$  and  $\Delta O = [(\langle (O - \bar{O})^2 \rangle_0)]^{1/2}$ .

The time-averaged density-matrix can be compared with the density-matrices of equilibrium ensembles. For an isolated system, one expects the microcanonical ensemble to hold at equilibrium with  $\rho_{\text{micro}} = \Omega^{-1} \sum_{n \in \Omega} |\phi_n\rangle \langle \phi_n|$ , where  $\Omega(\langle E \rangle, \Delta E)$  is the number of eigenstates within an energy window  $\langle E \rangle \pm \Delta E$  around the mean value  $\langle E \rangle$  fixed as an external parameter. The distribution can as well be compared with a canonical ensemble for which the  $p_n$  are the Boltzmann weights. Another possible one is the generalized Gibbs ensemble [3], suited for integrable systems and derived from

the maximization of the entropy with conserved quantities as constraints.

The difficulty for non-integrable systems is to compute the weights  $p_n$  or any expectation value. The solution is to resort to numerical techniques and we use LD in the following. First, we use the fact that the  $p_n$  enter in the expression of the (squared) fidelity [9]  $F(t) = |A(t)|^2 = \langle \rho(t) \rangle_0 = 1 - 4 \sum_{n < m} p_n p_m \sin^2[\Omega_{nm}t/2]$ , which is the revival probability after a time  $t$ . The trick [12] is to compute the Fourier transform  $A(\omega)$  of the  $A(t)$  function using frequency space methods. Since there is no finite broadening in LD, we have a direct access to the Lehmann representation  $A(\omega) = \sum_n p_n \delta(\omega - \omega_n + E_0)$ . All the information we need for the discussion of the statistical features of  $\bar{p}$  is included in  $A(\omega)$  since both the energies and the weights of the excited states contributing to the time evolution are obtained. Hilbert spaces of sizes up to  $10^7$  states will be studied in the following while full diagonalizations are restricted to  $10^4$  [13].

The short and long time behaviors of  $F(t)$  also carry some information about the  $p_n$  distribution [9]: at short times  $F(t) \simeq 1 - t^2/\tau^2$  with  $\tau^{-1} = \Delta E$ , the energy fluctuations. Physically,  $\tau$  is thus the time scale at which the system “escapes” from the initial state and it is the inverse of the centered width of  $A(\omega)$ . More generally, higher moments of the  $A(\omega)$  function are defined by  $M_q = \langle [\mathcal{H} - \langle \mathcal{H} \rangle_0]^q \rangle_0$ , and are clearly fixed by the initial state. In practice, the moments can be reliably computed with LD for  $q$  up to hundreds. Knowing all moments amounts to knowing the distribution itself and would give back  $\bar{p}$ . This remark was put forward without proof in Ref. 5. Hence, if one includes all moments as constraints to construct a density-matrix,  $\bar{p}$  will be recovered. However, moments with  $q \geq 3$  are physically meaningless since they cannot be measured, so they may not enter as constraints in a statistical description. Similarly, if  $\mathcal{H}$  is Gaussian, the energy and second moment are sufficient to reconstruct  $\bar{p}$ ; nevertheless, this is not a universal situation and may not be valid in strongly correlated model such as the BHM. At long times,  $F(t)$  usually fluctuates around its mean value  $\bar{F} = \sum_n p_n^2$  [13]. A qualitative interpretation of  $\bar{F}$  is the “participation ratio” [9] that counts the number of eigenstates that contribute during time evolution. The typical fluctuations of the fidelity are  $(\Delta F)^2 = \overline{F(t)^2} - \bar{F}^2 = 4 \sum_{n < m} p_n^2 p_m^2$ . This quantity qualitatively tells us whether the system prefers to stay close to the initial state or visit other states. In the thermodynamical limit,  $\bar{F}$  and  $\Delta F$  will not scale to zero unless  $A(\omega)$  has delta peaks with finite weights.

Qualitatively, a quench consists in preparing an initial state with some given Hamiltonian, and in projecting it onto the spectrum of the Hamiltonian governing the dynamics. Straightforward results from perturbation theory in the quench amplitude can be given to illustrate the difference between small and large quenches, and that a crossover on finite systems between the two regimes is expected on general grounds. Writing  $\mathcal{H} = \mathcal{H}_0 + \lambda \mathcal{H}_1$  with  $\lambda$  the quench amplitude and  $\mathcal{H}_1$  the perturbing operator, the perturbed weights read, for  $\lambda \ll 1$ ,  $p_0 \simeq 1 - \lambda^2 \sum_{n \neq 0} h_{n0}$ , and  $p_{n \neq 0} \simeq \lambda^2 h_{n0}$ , in which

the notation  $h_{n0} = |\langle \psi_n | \mathcal{H}_1 | \psi_0 \rangle|^2 / (E_n - E_0)^2$  has been used. Meanwhile, the  $\omega_n$  are slightly shifted to order  $\lambda$  and the eigenfunctions too. Hence, there is a transfer of spectral weight from the targeted ground-state  $|\psi_0\rangle$  to the other excited states. We get the scaling of several quantities to lowest order in  $\lambda$ :  $M_q \propto \lambda^2$ ,  $1 - \bar{F} \propto \lambda^2$  and  $\Delta F \propto \lambda^2$ . As  $\bar{F} > 0$ , these scalings will fail for  $\lambda$  of the order of unity. In addition, we mention that the mean-energy trivially scales, for any  $\lambda$ , with the quench amplitude  $\lambda$  since  $\langle E \rangle = \langle \mathcal{H} \rangle_0 = E_0 + \lambda \langle \mathcal{H}_1 \rangle_0$ . In a scenario in which the large amplitude limit is such that all weights are equal to  $\Omega^{-1}$ , as in the microcanonical ensemble, one has  $\bar{F} \propto \Omega^{-1}$  and  $\Delta F \propto \Omega^{-1}$ . The two types of scalings help to decide between the two regimes of the crossover.

*Application to a global quench in the one-dimensional Bose-Hubbard model* – We now study the BHM in a one-dimensional optical lattice that is known to be non-integrable:

$$\mathcal{H} = -J \sum_j [b_{j+1}^\dagger b_j + b_j^\dagger b_{j+1}] + U/2 \sum_j n_j(n_j - 1),$$

with  $b_j^\dagger$  the operator creating a boson at site  $j$  and  $n_j = b_j^\dagger b_j$  the local density.  $J$  is the kinetic energy scale while  $U$  is the magnitude of the onsite repulsion. In an optical lattice, the ratio  $U/J$  can be tuned by changing the depth of the lattice and using Feshbach resonance [1]. When the density of bosons is fixed at  $n = 1$  and  $U$  is increased, the equilibrium phase diagram of the model displays a quantum phase transition from a superfluid phase to a Mott insulating phase in which particles are localized on each site. The critical point has been located at  $U_c \simeq 3.3J$  using numerics [14]. The quenches are performed by changing the interaction parameter  $U_i \rightarrow U_f$  (we set  $J = 1$  in the following), so we have  $\lambda = (U_f - U_i)/2$ , and the perturbing operator  $\mathcal{H}_1 = \sum_j n_j(n_j - 1)$  is diagonal. Numerically, one must fix a maximum onsite occupancy. We take four as in Ref. 4 (for further details, see [13]).

Since  $\bar{p}$  features a mixed state, we call the  $(U_i, U_f)$  plane a state diagram. The  $U_i = U_f$  line splits this state diagram in

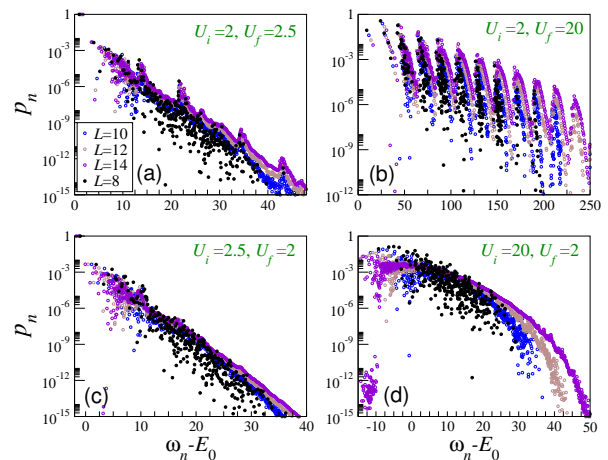


FIG. 1: (Color online) Distributions of the  $p_n$  at four different points of the  $(U_i, U_f)$  states diagram. For the smallest size  $L = 8$ , exact results are obtained by full diagonalization.

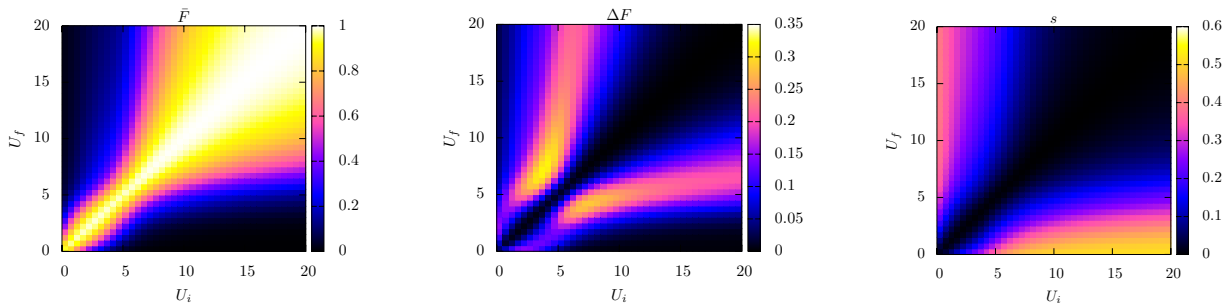


FIG. 2: (Color online) Maps of the observables  $\bar{F}$ ,  $\Delta F$  and entropy per particle  $s$  characterizing the time-averaged density-matrix  $\bar{\rho}$ . Results are obtained by LD on a finite system ( $L = 12$ ) with periodic boundary conditions.

two regions and the previous perturbative arguments should hold close to this line. Moreover, if the equilibrium critical point  $U_c$  plays a role, it will split it into six regions according to the lines  $U_i = U_c$  and  $U_f = U_c$ , depending on whether the targeted ground-state  $|\phi_0\rangle$  is in the same phase as  $|\psi_0\rangle$  or not. In Fig. 1, we give the typical distributions of the weights versus energy for four points of the state diagram: two with small quenches within the same (superfluid) phase and two for large quenches that cross  $U_c$  in both directions. We observe that in the first two situations, the distributions are close to an exponential decay typical of a *canonical* ensemble. This looks surprising for a closed system but, on the other hand, in the perturbative regime, the momenta  $M_q$  of the energy distribution are negligible w.r.t.  $\langle E \rangle - E_0$ . Hence, if one optimizes the entropy  $S$  with only the energy  $\langle E \rangle$  as a constraint, one finds a Boltzmann law behavior  $p_n \propto e^{-\beta\omega_n}$ . Taking higher momenta into account would yield corrections to this Boltzmann law. However, we see, for instance, that some peaks emerge in the distribution for  $(U_i = 2, U_f = 2.5)$ . Indeed, for the two large quenches, the distributions are strongly different from either the microcanonical or the canonical ensemble. When  $U_f = 20$ , Mott excitations, corresponding to doubly occupied sites and roughly separated by  $U_f$ , are clearly visible in the spectrum. Although the overall decay of the  $p_n$  is exponential, the distribution is very different from a Boltzmann law. This explains that many observables differ from the ones of an equilibrium system as observed in Ref. 4. When  $U_f = 2$ , the targeted spectrum is nearly continuous and the distribution displays strong weights around zero energy and a subexponential behavior [something like  $\exp(-(\omega_n - E_0)^\gamma)$  with  $\gamma > 1$ ]. This is again different from equilibrium predictions. The bump-like shape of the  $U_f = 2$  distribution in Fig. 1 can be qualitatively understood from the fact that the ground-state energy increases with  $U$  in the BHM. As  $E_0 > \omega_0$  when  $U_f < U_i$ , the initial state is close in energy to some excited states of  $\mathcal{H}$  which may favor their excitations by the quenching process, according to the perturbative form of the  $p_n$ . Another consequence is that the state diagram is expected to be non-symmetrical w.r.t. the  $U_i = U_f$  line. To sketch the state diagram, maps of integrated quantities such as  $\bar{F}$ ,  $\Delta F$ , and the entropy per particle  $s = S[\bar{\rho}]/N$  (we find that the entropy is extensive) are computed on a finite system with  $L = 12$

and given in Fig. 2. As suggested previously, observables display a strong crossover from the perturbative regime to a non-perturbative regime characterized by a strong enhancement of the weights of excited states.

In order to evaluate the finite size effects on the crossover, we look at the scalings of  $\bar{F}$  and  $\Delta F$  for a cut along the  $U_i = 2$  line and increasing  $\lambda$ . We may wonder whether there is a singular point separating the two regimes, and second, if the equilibrium critical point plays a role.  $\bar{F}$  goes from 1 when  $\lambda = 0$  to zero (in the thermodynamical limit), when  $\lambda$  is large [13]. The second derivative  $d^2\bar{F}/d\lambda^2$  crosses zero on a finite system for a value  $\lambda_c(L)$  and we define the corresponding  $\bar{F}_c = \bar{F}(\lambda_c(L))$ . The scalings with  $1/L$  of these two quantities are given in the EPAPS: a linear scaling suggests that they are finite in the thermodynamical limit but power-law scalings going to zero also works for both, so studying this quantity is not conclusive. More interestingly,  $\Delta F$  increases with  $L$ , and as  $\lambda^2$  in the perturbative regime, but decreases with  $L$  in the large  $\lambda$  limit (see Fig. 3). It passes through a maximum that defines a new  $\lambda_c(L)$ , and the corresponding  $\Delta F_c = \Delta F(\lambda_c(L))$ . The scaling of this  $\lambda_c(L)$  suggests a finite value in the thermodynamical limit.  $\Delta F_c$  can scale to a finite value but also to zero as a power-law. Yet, the latter situation would be in contradiction with a finite  $\lambda_c$  and the fact that  $\Delta F$  increases with  $L$  at low  $\lambda$ , so the results suggest that there is a singular point (in the sense of the maximum of  $\Delta F$ ) separating the two regimes. Three other cuts are given in the EPAPS which support the same increase of  $\Delta F$  with  $L$  in the perturbative regime. Next, we can define the “equilibrium expectation”  $\lambda_c^{eq} = (U_c - U_i)/2$  [resp.  $(U_f - U_c)/2$ ] if one scans over  $U_f$  [resp.  $U_i$ ] and compare it with the scalings of actual  $\lambda_c$ . In Fig. 3, the two are too close to be conclusive but for large  $U_{i,f}$  [13], the difference is much substantial as the maxima of  $\Delta F$  scales away from  $\lambda_c$ . We thus infer that  $U_c$  certainly plays a role (see below) but not on the crossover.

We now discuss some of the thermodynamical features of the mixed states described by the density-matrix  $\bar{\rho}$ . First, we ask whether the averaged energy is well-defined by looking at the relative energy fluctuations defined as  $\frac{\Delta E}{E} \equiv \frac{\Delta E}{(\langle E \rangle - E_0 + \lambda N)} = \sqrt{\frac{\sum_{ij} \langle n_i^2 n_j^2 \rangle_0 - \langle n_i^2 \rangle_0 \langle n_j^2 \rangle_0}{\sum_i \langle n_i^2 \rangle_0}}$  to get rid of the triv-

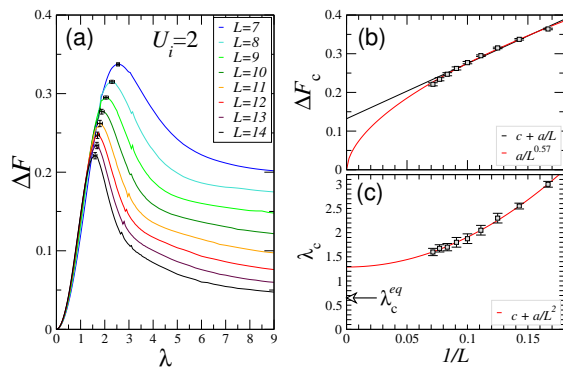


FIG. 3: (Color online) (a) Cut along the  $U_i = 2$  line of  $\Delta F$  showing a maximum between the perturbative and large quench regimes. (b-c) Finite size scalings of  $\Delta F_c$  and  $\lambda_c$ . See text for discussion.

ial dependencies of  $\langle E \rangle$  on  $E_0$ ,  $N$  and  $\lambda$ : what remains are the relative “squared density” fluctuations in the initial state. In the superfluid phase, we expect the squared density-density correlations to have an algebraic behavior  $\langle n_i^2 n_j^2 \rangle_0 - \langle n_i^2 \rangle_0 \langle n_j^2 \rangle_0 \sim |i - j|^{-\alpha}$ , while they should be exponential in the Mott phase  $e^{-|i-j|/\xi}$ , with  $\xi$  the correlation length. On a chain of length  $L$ , we thus have  $\Delta E = \lambda \sqrt{L} g(L)$  with: (i) if  $\alpha < 1$ , then  $g(L) \sim L^{(1-\alpha)/2}$ , (ii) if  $\alpha = 1$ ,  $g(L) \sim \sqrt{\ln L}$  and if  $\alpha > 1$  or  $\xi > 0$ ,  $g(L) = \text{const}$ . As we have  $\alpha > 1$  in the superfluid phase of the 1D BHM [15] and  $\sum_i \langle n_i^2 \rangle_0 \sim L$ , we find that  $\Delta E/E \sim f(U_i)/\sqrt{L}$  for any  $U_i$ . The  $f(U_i)$  function is plotted in Fig. 4 which shows a very good agreement with this argument and, as expected, a decrease with  $U_i$  as the density fluctuations are reduced. This  $1/\sqrt{L}$  scaling is similar to the one in (micro)canonical ensembles but one also notes that starting from an initial state with strong density fluctuations ( $\alpha \leq 1$ ) yields an anomalous scaling of the relative energy fluctuations. In the BHM, this can be achieved by introducing nearest neighbor repulsion [14]. We also get the scaling  $\tau \sim \lambda^{-1} L^{-1/2}$  which shows that, even if  $\tau$  scales to zero in the thermodynamical limit, it can be significantly long on large but finite systems for small  $\lambda$ . More importantly, we find that two mixed states  $\bar{\rho}$  can have the same energy  $\langle E \rangle$  but with different  $\lambda$  so that they do not originate from the same initial state and consequently, have different energy fluctuations. As energy fluctuations could be measured, one can argue that, in that sense,  $\bar{\rho}$  keeps a memory on the initial state. In addition, we give, in Fig. 2, the entropy per particle  $s$  that increases monotonically with  $\lambda$  and reveals more significantly the underlying anisotropy of the states diagram. The mixed state also keeps memory of the initial state through its entropy.

In conclusion, we have shown that the weights of the time-averaged density-matrix  $\bar{\rho}$  can be obtained with LD. This provides an observable-free description of the quench process in non-integrable systems. It is shown that there is a clear crossover from a perturbative regime in which the distribution is Boltzmann-like to distributions that are not predicted by equilibrium statistics. The argument and the approach are generic. The method is applied to the 1D BHM for which the

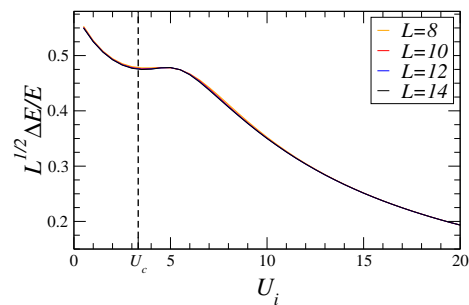


FIG. 4: (Color online) Rescaled relative energy fluctuations in the mixed state. They only depend on the features of the initial state. The slope of the curves vanishes close to the equilibrium critical point  $U_c$ .

state diagram has been mapped in the  $(U_i, U_f)$  plane. In addition, finite size effects have been addressed and the mixed state is shown to have a well defined energy and to keep a memory of the initial state through the energy fluctuations or the entropy.

I thank T. Barthel, F. Heidrich-Meisner, T. Jolicoeur, D. Poilblanc and D. Ullmo for fruitful discussions.

\* Electronic address: guillaume.roux@u-psud.fr

- [1] M. Greiner, O. Mandel, T. W. Hänsch, and I. Bloch, *Nature* **419**, 51 (2002); T. Kinoshita, T. Wenger, and D. S. Weiss, *Ibid.* **440**, 900 (2006); S. Hofferberth, I. Lesanovsky, B. Fischer, T. Schumm, and J. Schmiedmayer, *Ibid.* **449**, 324 (2007).
- [2] R. Schützhold, M. Uhlmann, Y. Xu, and U. R. Fischer, *Phys. Rev. Lett.* **97**, 200601 (2006); M. A. Cazalilla, *Ibid.* **97**, 156403 (2006); P. Calabrese and J. Cardy, *Ibid.* **96**, 136801 (2006); M. Eckstein and M. Kollar, *Ibid.* **100**, 120404 (2008); F. Heidrich-Meisner, M. Rigol, A. Muramatsu, A. E. Feiguin, and E. Dagotto, *Phys. Rev. A* **78**, 013620 (2008).
- [3] M. Rigol, V. Dunjko, V. Yurovsky, and M. Olshanii, *Phys. Rev. Lett.* **98**, 050405 (2007).
- [4] C. Kollath, A. M. Läuchli, and E. Altman, *Phys. Rev. Lett.* **98**, 180601 (2007).
- [5] S. R. Manmana, S. Wessel, R. M. Noack, and A. Muramatsu, *Phys. Rev. Lett.* **98**, 210405 (2007).
- [6] M. Rigol, V. Dunjko, and M. Olshanii, *Nature* **452**, 854 (2008).
- [7] M. Kollar and M. Eckstein, *Phys. Rev. A* **78**, 013626 (2008).
- [8] M. Cramer, C. M. Dawson, J. Eisert, and T. J. Osborne, *Phys. Rev. Lett.* **100**, 030602 (2008); T. Barthel and U. Schollwöck, *Ibid.* **100**, 100601 (2008); M. Cramer, A. Fleisch, I. P. McCulloch, U. Schollwöck, and J. Eisert, *Ibid.* **101**, 063001 (2008).
- [9] A. Peres, *Phys. Rev. A* **30**, 1610 (1984); *Ibid.* **30**, 504 (1984).
- [10] P. Reimann, preprint, arXiv:0810.3092.
- [11] A. Silva, *Phys. Rev. Lett.* **101**, 120603 (2008); A. Polkovnikov, preprint, arXiv:0806.0620.
- [12] F. Mila and D. Poilblanc, *Phys. Rev. Lett.* **76**, 287 (1996).
- [13] See the EPAPS file online.
- [14] T. D. Kühner, S. R. White, and H. Monien, *Phys. Rev. B* **61**, 12474 (2000).
- [15] T. Giamarchi, *Quantum Physics in One Dimension* (Oxford University Press, Oxford 2004).

# ELECTRONIC PHYSICS AUXILIARY PUBLICATION SERVICE FOR: ON QUENCHES IN NON-INTEGRABLE QUANTUM MANY-BODY SYSTEMS: THE ONE-DIMENSIONAL BOSE-HUBBARD MODEL REVISITED

## Typical behavior of the fidelity with time

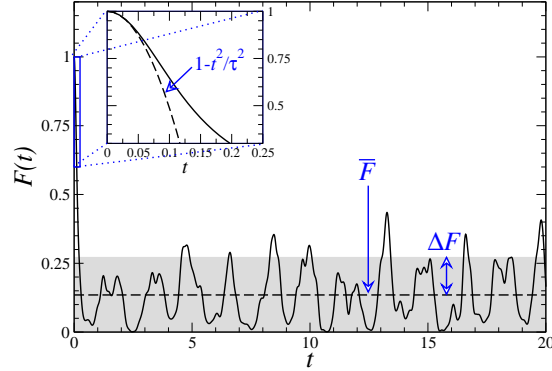


FIG. 5: Typical behavior of the fidelity for a finite size system with  $L = 10$  starting from  $U_i = 2$  to  $U_f = 8$  ( $\lambda = 3$ ). At short times:  $F(t) = 1 - t^2/\tau^2$  (here  $\tau = 0.14$ ). For long times,  $F(t)$  fluctuates around its mean value  $\bar{F}$  (here  $\bar{F} = 0.135$  and  $\Delta F = 0.136$ ).

## Technical details on Lanczos calculations

We use 200 Lanczos iterations to get the ground state and 1200 to get the Lehmann representation of  $A(\omega)$ . We do not use symmetries of the Hamiltonian except particle number conservation. With periodic boundary conditions, translational symmetries induce some selection rules for the  $p_n$  so their number is quite reduced. We have checked that Lanczos gives a good result by comparing it with exact results obtained by full diagonalization on a system with  $L = 8$  (see Fig. 6). The largest Hilbert space size is 13311000 for  $L = 14$  for Lanczos diagonalization and 5475 for  $L = 8$  for full diagonalization. Very similar results are obtained from systems with open boundary conditions.

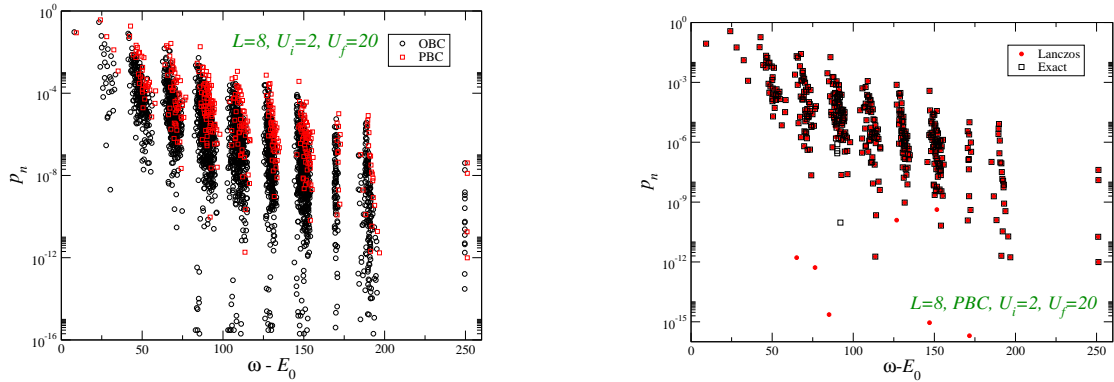


FIG. 6: Test on symmetries and effect of boundary conditions on the distribution of the  $p_n$ . PBC stands for periodic boundary conditions while OBC is for open BC.

## Additional results on the Bose-Hubbard model

Moments are related to the  $p_n$  and  $\omega_n$  through  $M_q = \sum_n p_n [\omega_n - \langle E \rangle]^q$ . They undergo a clear change of behavior with  $\lambda$  as shown in Fig. 7.



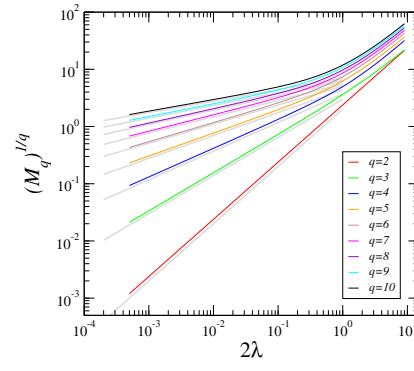


FIG. 7: First moments  $M_q$  (to the power  $1/q$ ) of the  $A(\omega)$  function for a system with  $L = 10$  and  $U_i = 2$ . There is a crossover from the perturbative result  $M_q \sim \lambda^2$  to a regime where  $M_q \sim \lambda^q$  at large  $\lambda$ .

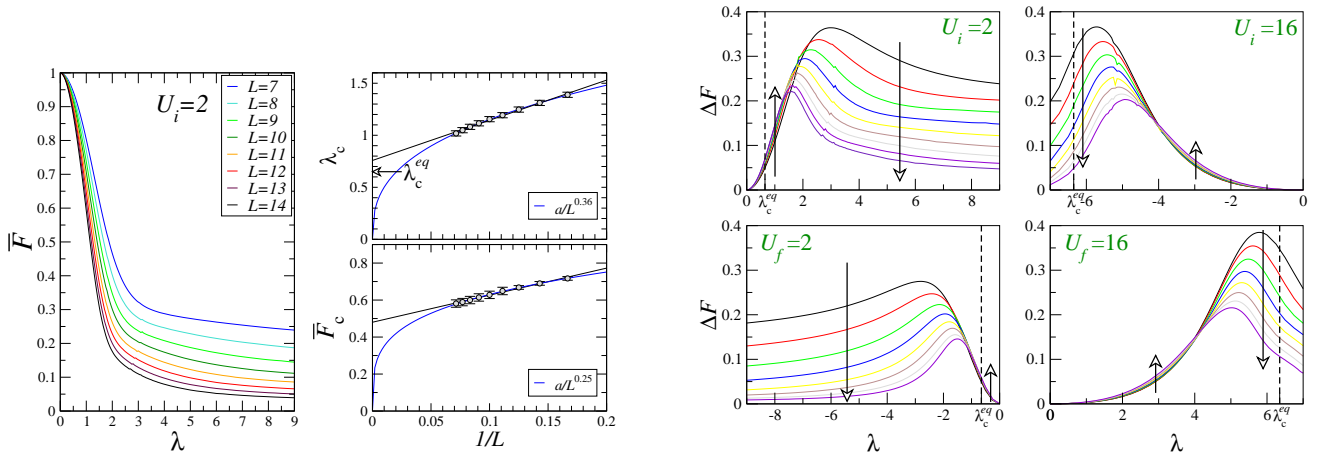


FIG. 8: *Left*: Cut along the  $U_i = 2$  axis of  $\bar{F}$ . A linear scaling gives both a finite value for  $\bar{F}_c$  and  $\lambda_c$  but a power-law one (going to zero) is also plausible. *Right*: Four cuts in the state diagram showing the scaling behavior of  $\Delta F(L)$  as a function of  $\lambda$ . The smallest size is  $L = 6$  and larger  $L = 13$  except for  $U_i = 2$  for which it is  $L = 14$ . Results for  $L = 6, 7, 8$  are *exact* (full diagonalization) while larger sizes are obtained with Lanczos. The arrows indicate how  $\Delta F$  increases or decreases with  $L$ .